

Phase Transition and Electrical Properties of $\text{Ba}_{0.7}\text{Ca}_{0.3}\text{TiO}_3\text{--BiFeO}_3$ CeramicsCai-Xia Li,^{‡,§} Bin Yang,^{‡,†} Shan-Tao Zhang,^{¶,†} Feng-Min Wu,[‡] and Wen-Wu Cao^{||}[‡]Department of Physics, Center for Condensed Matter Science and Technology, Harbin Institute of Technology, Harbin 150001, China[§]Department of Material and Physics, School of Applied Sciences, Harbin University of Science and Technology, Harbin 150080, China[¶]Department of Materials Science and Engineering & National Laboratory of Solid-State Microstructures, Nanjing University, Nanjing 210093, China^{||}Materials Research Institute, The Pennsylvania State University, University Park, Pennsylvania 16802

Lead-free piezoelectric ceramics of $(1-x)\text{Ba}_{0.70}\text{Ca}_{0.30}\text{TiO}_3\text{--}x\text{BiFeO}_3$ [$(1-x)\text{BCT--}x\text{BF}$, $x = 0\text{--}0.065$] have been prepared and investigated. The ceramics with $x \leq 0.06$ have diphasic tetragonal and orthorhombic crystal structures, whereas tetragonal phase is suppressed by the introduction of BF. As a result, the composition with $x = 0.065$ is found to have diphasic pseudocubic and orthorhombic phases. Significantly composition-dependent grain size is observed. With increasing x from 0 to 0.065, the ferroelectric-paraelectric phase transition temperature decreases monotonically from 128°C to 50°C, accompanied by enhanced ferroelectric relaxor behavior, as indicated by the widened diffused phase transition temperature. The room temperature polarization–electric field (P – E) hysteresis loops and strain–electric field (S – E) curves indicate that the ferroelectricity enhances slightly and reaches the maximum near $x = 0.05$, and then weakens with increasing x . On the other hand, the piezoelectric coefficient (d_{33}) and electromechanical coupling coefficient (k_p) decrease simultaneously with increasing x , whereas the mechanical quality factor (Q_m) reaches the maximum near $x = 0.05$. The structure-property relationship is discussed intensively. Our results may be helpful for further understanding and designing BaTiO_3 -related lead-free ferroelectric/piezoelectric materials.

I. Introduction

BARIUM titanate, BaTiO_3 (BT) is the one of the most important perovskite-type ferroelectric materials, its ferroelectric-paraelectric phase transition temperature (Curie temperature, T_c) is around 120°C.¹ BT-based solid solutions have been intensively studied in to enhance the dielectric, ferroelectric and piezoelectric properties,^{2–4} which are important for applications in various electronic devices. Among the reported solid solutions, $\text{BaTiO}_3\text{--CaTiO}_3$ (BT–CT) are of particular interests because of some special features.^{5–12} First, this system has a solubility limit for CT of around 0.23, and diphasic tetragonal and orthorhombic structures above the solubility limit.^{8,9} Second, the introduction of CT causes a negligible change of T_c ,⁸ but strongly lowers the tetragonal–orthorhombic transition temperature, improves the temperature reliability of dielectric and piezoelectric property

greatly.^{10–12} And third, a relaxation behavior has been generally observed in many B-site substituted BT such as $\text{Ba}(\text{Ti},\text{Sn})\text{O}_3$,¹³ $\text{Ba}(\text{Ti},\text{Ce})\text{O}_3$,¹⁴ and $\text{Ba}(\text{Ti},\text{Zr})\text{O}_3$,¹⁵ however, rarely observed in A-site substituted BT. For example, the dielectric constant–temperature curves of BT–CT solid solutions have sharp phase transition peaks, indicating the negligible relaxor characteristics.¹⁶

Moreover, composite and diphasic materials have been known to possess the potential for performance far beyond those of constituent materials.⁸ Fu and Cohen reported that high strain of the ultrahigh electrostriction materials like $\text{Pb}(\text{Zn}_{1/3}\text{Nb}_{2/3})\text{TiO}_3\text{--PbTiO}_3$ (PZN–PT) was resulted from the coupling between two equivalent energy states, i.e., the tetragonal and rhombohedral phases.¹⁷ Wang *et al.* reported that the dielectric constant in the composite phase ($x = 0.23\text{--}0.40$) of $\text{Ba}_{1-x}\text{Ca}_x\text{TiO}_3$ (BCT) ceramics was higher than that in the pure ferroelectric phase, higher electrostrictive strain of 0.22%, higher ferroelectric, and higher piezoelectric properties were obtained in the diphasic BCT ceramics near the solubility limit, and it was suggested that the interaction between the ferroelectric tetragonal phase and the dielectric orthorhombic phase acted as an important factor in improving ceramic properties.⁸ Li *et al.* reported that the high piezoelectric properties ($d_{33} \sim 510$ pC/N) in $\text{Ba}_{0.98}\text{Ca}_{0.02}(\text{Ti}_{0.96}\text{Sn}_{0.04})\text{O}_3$ ceramics was ascribed to the phase coexistence and the polymorphic phase transition (PPT) occurring near room temperature.³ And in view of high piezoelectricity ($d_{33} \sim 620$ pC/N) in Pb-free piezoelectric ceramic system $\text{Ba}(\text{Ti}_{0.80}\text{Zr}_{0.20})\text{O}_3\text{--Ba}_{0.70}\text{Ca}_{0.30}\text{TiO}_3$ reported by Liu and Ren,² which possesses a triple point in the phase diagram. So it will be very interesting to investigate $\text{Ba}_{0.70}\text{Ca}_{0.30}\text{TiO}_3$ diphasic ceramics which is near the solubility limit of BCT ceramics, and an effective way to develop high-performance Pb-free piezoelectrics by forming a suitable phase boundary.

On the other hand, BiFeO_3 (BF) is a rare single phase material with ferroelectric ($T_c \sim 827^\circ\text{C}$) and antiferromagnetic ($T_N \sim 367^\circ\text{C}$) orders simultaneously.^{18,19} It is expected that the introduction of BF into BT can lead to relaxor behavior because such introduction equals to the A-site and B-site co-substitutions. In addition, adding BF can lead to denser BT-based ceramics, and thus affect the phase transition, dielectric, ferroelectric, and piezoelectric properties.²⁰

According to the above descriptions, to obtain excellent dielectric, ferroelectric, and piezoelectric properties and high T_c , in this article we present details of how we prepared the ceramics of $(1-x)\text{Ba}_{0.70}\text{Ca}_{0.30}\text{TiO}_3\text{--}x\text{BiFeO}_3$ (BCT–BF; $x = 0\text{--}0.065$) and investigated the structures and electric properties as the functions of composition. Composition-dependent relaxor behavior, ferroelectric, and piezoelectric properties were discussed based on composition-dependent structure.

D. D. Viehland—contributing editor

Manuscript No. 31405. Received April 29, 2012; approved July 08, 2012.

[†]Authors to whom correspondence should be addressed. e-mails: binyang@hit.edu.cn and stzhang@nju.edu.cn

II. Experimental Procedure

Using a conventional solid-state reaction method, BCT–BF ($x = 0–0.065$) ceramics were prepared. Regent grade BaCO_3 (99.0%), CaCO_3 (99.0%), TiO_2 (99.0%), Bi_2O_3 (99.9%), and Fe_2O_3 (99.99%) were weighed according to the chemical formula of $(1-x)\text{BCT}-x\text{BF}$ ($x = 0, 0.005, 0.01, 0.02, 0.03, 0.04, 0.045, 0.05, 0.055, 0.06, \text{ and } 0.065$). After being ball-milled in alcohol for 12 h using agate balls in planetary mill, each slurry was dried, and then calcined at 1100°C for 3 h. The calcined powders were ball-milled again for 16 h to obtain homogeneous powder. Disks of 13 mm in diameter and 0.6–1 mm in thickness were pressed using 8% polyvinyl alcohol binder under pressure of 100 MPa. The binder was burnt out by slow heating at 550°C for 2 h. The sintering was conducted between 1250°C and 1400°C in air for 1 h, lower temperature for the higher BF content, followed by a furnace cooling. The samples were embedded in the same compositional powder during sintering to reduce the volatility of Bi. All the samples had relative densities higher than 94%.

The phases of ceramics were identified using X-ray diffraction (XRD) on grounded, unpoled samples with an automated Rigaku D/max 2400 X-ray diffractometer (Rigaku Corporation, Tokyo, Japan) using $\text{CuK}\alpha$ radiation. The microstructures were observed using a back-scattered scanning electron microscopy (SEM; Quanta 200FEG, FEI Corporation, OR). For electric measurements, the sintered disks were grounded carefully to ensure parallel surfaces. The circular surfaces of the disks were covered with a thin layer of silver paste and fired at 600°C for 30 min. The temperature dependence of dielectric property was measured at different frequencies between 0.1 and 1000 kHz with an Agilent (Agilent Technologies, CA) E4980A LCR meter. The room temperature ferroelectric polarization–electric field (P – E) hysteresis loops and bipolar strain–electric field (S – E) curves were measured at 1 Hz with precision premier II (Radiant Technology Inc., NM) in silicone oil. For piezoelectric measurement, the samples were poled with the field of 30 kV/cm for 20 min at the temperature of 20°C – 100°C in a silicone oil bath. The piezoelectric constant d_{33} was measured using a quasi-static d_{33} meter (Institute of Acoustics, Chinese Academy of Sciences, ZJ-4A, China). The planar electromechanical coupling factors k_p and the mechanical quality factor Q_m were measured using a resonance-antiresonance method using an impedance analyzer (Agilent 4294A) and calculated following IEEE standards.

III. Results and Discussion

Figure 1 shows the XRD patterns of the BCT–BF ceramics. The ceramics with $x \leq 0.06$ show coexisted tetragonal and orthorhombic phases without any other impurity phases, consistent with other report,^{5,8,9} suggesting that BF can enter into the lattice of BCT to form stable solid solutions. More interestingly, the ceramics with $x \leq 0.06$ have a tetragonal symmetry

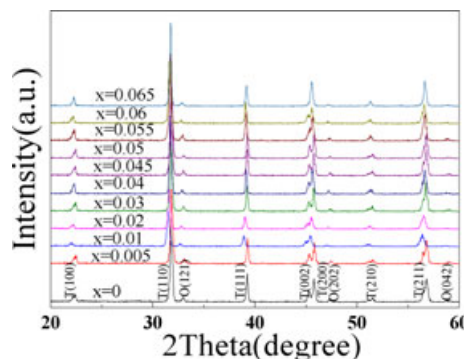


Fig. 1. X-ray diffraction (XRD) patterns of $(1-x)\text{BCT}-x\text{BF}$ ceramics ($x = 0–0.065$).

as evidenced by the splitting of the (002)/(200) peaks at 2θ – 46° ,²¹ however, the tetragonal structure gradually diminishes with increasing BF content, and the split (002)/(200) peaks of the tetragonal phase finally merge into a single (200) peak at $x = 0.065$, suggesting that the crystal structure of the BCT–BF ceramics evolves from the tetragonal–orthorhombic phases coexistence to a pseudocubic–orthorhombic diphasic phases. In other words, BF mainly enters into the tetragonal phase of the BCT ceramics, one of the possible reasons is that the tetragonal phase is dominant in BCT ceramics, which is evidenced by the relative peaks of tetragonal phase and orthorhombic phase according to the XRD and the change of the grain size from the microstructure SEM images (Fig. 2).

All ceramics show dense microstructures, the typical back-scattered field emission SEM images of the BCT–BF ceramics with $x = 0.01, 0.02, 0.03, 0.04, 0.05, \text{ and } 0.06$ are shown in Fig. 2, and the energy-dispersive X-ray spectrometry observations show that the small orthorhombic phase grains disperse among the larger tetragonal phase grains matrix, consistent with the coexistence of tetragonal and orthorhombic phases in BCT ceramics shown in the XRD data (Fig. 1) and with the previous report.⁸ In general, it can be seen that the grain size of tetragonal phase, varying between 1 and $6.5 \mu\text{m}$, increases significantly with increasing BF content, however, the content

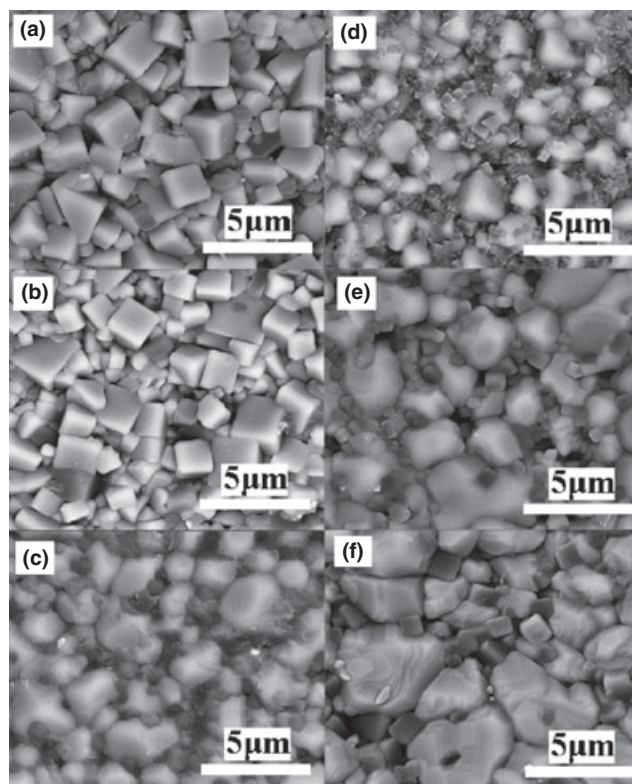


Fig. 2. SEM micrographs of $(1-x)\text{BCT}-x\text{BF}$ ceramics sintered at 1250°C for 1 h (a) $x = 0.01$, (b) $x = 0.02$, (c) $x = 0.03$, (d) $x = 0.04$, (e) $x = 0.05$, and (f) $x = 0.06$.

Table I. Grain Size of $(1-x)\text{BCT}-x\text{BF}$ ($x = 0–0.065$) Ceramics

x	Grain size (T) (μm)	Grain size (O) (μm)
0	1.0	0.81
0.01	1.2	0.85
0.02	2.3	0.83
0.03	2.6	0.87
0.04	2.7	0.86
0.05	3.0	0.89
0.06	5.4	0.89
0.065	6.5	0.88

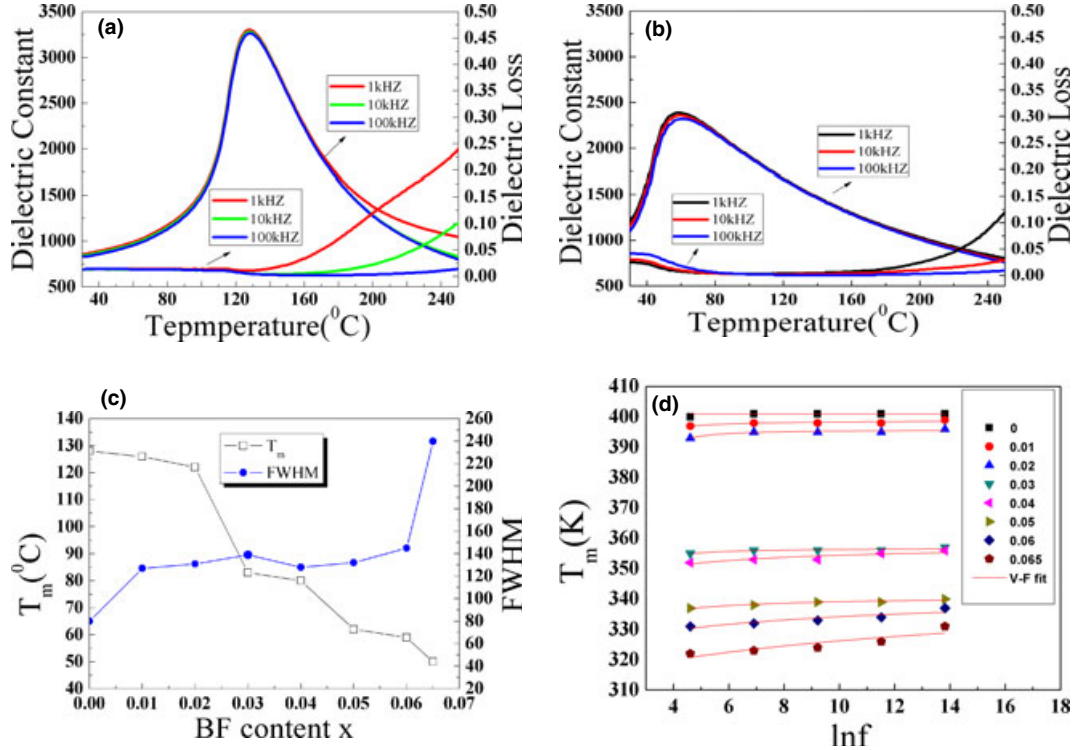


Fig. 3. Temperature-dependent dielectric properties of the $(1-x)\text{BCT}-x\text{BF}$ ceramics (a) $x = 0$, (b) $x = 0.06$, (c) T_m and FWHM of the $(1-x)\text{BCT}-x\text{BF}$ ceramics as a function of BF content, and (d) The plots of T_m versus $\ln f$ and the fitted curves.

of the orthorhombic phase keeps almost constant, which is shown in Table I. This again indicates that the effects of BF mainly act on tetragonal phases. And the XRD shows the decreased internal stress which may be related to the increased grain size of tetragonal phase, and the decreased internal stress may result in more obvious diffused phase transition and the decreased Curie temperature.

Figures 3(a) and (b) show the temperature dependence of the relative dielectric permittivity (ϵ_r) and dissipation factor tangent ($\tan \delta$) measured at various frequencies for the composition with $x = 0$ and $x = 0.06$, respectively. Two features could be detected. First, the temperature corresponding to the dielectric maximum (T_m) decreases with increasing x value, as plotted in Fig. 3(c). This observation means that the introduction of BF decreases the ferroelectric–paraelectric phase transition temperature, consistent with other BT-based solid solutions.²² Second, as can be seen from Figs. 3(a) and (b), the composition with $x = 0$ has sharp T_c around 128°C and the T_c is frequency independent. For the composition with $x = 0.06$, the ϵ_m “peak” is broadened and the T_c is around 59°C which is frequency dependent. With increasing x , the phase transition becomes diffused, as evidenced by the fact that the temperature corresponding to the maximum relative dielectric constant (T_m) tends to be frequency dependent, i.e., shifting to higher temperature with increasing frequency, and the ϵ_m “peak” tends to be broadened with increasing x , indicated by the increased full width at the half maximum–minimum values (FWHM) of the ϵ_m at 1 kHz, as plotted in Fig. 3(c). Correspondingly, a dissipation factor peak is observed and shows the similar frequency and composition dependence. This feature confirms that the introduction of BF not only decreases the phase transition temperature but also causes the relaxor of BCT and the relaxor degree increases with increasing BF content. To analyse the effect of the BF content on the relaxation characters of BCT ceramics, the well-known Vogel–Fulcher formula is described as follows²³:

$$f = f_0 \exp \left[\frac{-E_a}{k_B(T_m - T_f)} \right] \quad (1)$$

where f is the measurement frequency, f_0 is the pre-exponential factor, E_a is the activation energy describing the polarization fluctuations of an isolated cluster relaxation process, T_m is the dielectric maximum in absolute temperature (K), T_f is the Vogel–Fulcher freezing temperature, and k_B is the Boltzmann constant. The plot of T_m versus $\ln(f)$ and the fitting curves are given in Fig. 3(d). The fitting parameters are summarized in Table II. It is clearly seen that the freezing temperature T_f decreases with increasing BF content. The decrease of T_f values indicates that the relaxor behavior of BCT–BF ceramics is enhanced with increasing BF content. And the degree of the relaxor behavior could be estimated by the empirical parameter ΔT_{relax} defined as⁷:

$$\Delta T_{\text{relax}} = T_{\text{max}(1000 \text{ kHz})} - T_{\text{max}(0.1 \text{ kHz})} \quad (2)$$

where $T_{\text{max}(1000 \text{ kHz})}$ and $T_{\text{max}(0.1 \text{ kHz})}$ are the temperatures corresponding to the dielectric constant maximum at frequencies of 1000 and 1 kHz, respectively. So, the calculated ΔT_{relax} values are 1°C, 2°C, 3°C, 4°C, 4°C, 4°C, 6°C, and 9°C for $x = 0, 0.01, 0.02, 0.03, 0.04, 0.05, 0.06$, and 0.065, respectively. So the degree of relaxor behavior is slightly dependent on BF content in BCT–BF ceramics.

According to the literature,^{7,22} a broadened dielectric permittivity peak with frequency dependence was observed in

Table II. Summary of the Vogel–Fulcher Fitting Parameters of the $(1-x)\text{BCT}-x\text{BF}$ ($x = 0-0.065$) Ceramics

x	E_a (meV)	f_0 (Hz)	T_f (K)
0	3.905	2.345×10^{10}	398
0.01	3.879	1.094×10^{10}	395
0.02	3.877	1.044×10^{10}	388
0.03	3.874	1.024×10^{10}	353
0.04	3.312	3.605×10^8	349
0.05	3.494	3.616×10^8	334
0.06	3.160	4.486×10^7	328
0.065	2.942	1.454×10^7	319

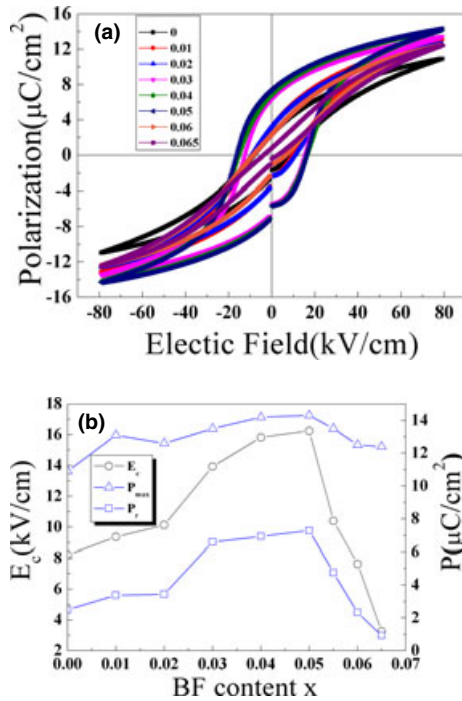


Fig. 4. (a) P - E hysteresis loops of $(1-x)\text{BCT}-x\text{BF}$ ($x = 0-0.065$) ceramics, (b) P_{\max} , P_r , and E_c values of $(1-x)\text{BCT}-x\text{BF}$ ceramics as a function of BF content.

Bi-doped $\text{Ba}_{1-x}\text{Ca}_x\text{TiO}_3$ ceramics, and it was suggested that Bi^{3+} ions were located at off-center positions of A-site, similarly as suggested for Ca doped SrTiO_3 and Bi-doped $\text{Ba}(\text{Zr}_x\text{Ti}_{1-x})\text{O}_3$.²² Therefore, A-site vacancies (V''_{A}) may appear to compensate the charge imbalance arising from the substitution of A-sites by Bi^{3+} ions. Off-center Bi^{3+} ions and $\text{Bi}^{3+}-V''_{\text{A}}$ centers form dipoles and further set up local random electric fields.⁷ These factors are believed to be

responsible for the suppressed ferroelectricity, decreased phase transition temperature, and enhanced ferroelectric relaxor behavior in $\text{Ba}_{1-x}\text{Ca}_x\text{TiO}_3$ ceramics.^{7,22} In the cases of our BCT-BF system, the substitution of A-sites by Bi^{3+} ions, together with the additional B-site Fe^{3+} substitution create charge imbalance, which must be compensated by either cation vacancies on the A-site or B-site (ionic compensation), or by electrons (electronic compensation). So, the similar effect may disrupt the long-range ordering of $\text{Ba}_{0.70}\text{Ca}_{0.30}\text{TiO}_3$, resulting in the enhanced relaxor behavior.

Figure 4(a) presents the room temperature P - E hysteresis loops of the $(1-x)\text{BCT}-x\text{BF}$ ceramics ($x = 0-0.065$) measured with the applied field of 80 kV/cm. Typical ferroelectric P - E hysteresis loops were observed for the ceramics with $x \leq 0.06$, which were significantly slim “loop.” The composition-dependent maximum polarization (P_{\max}), remnant polarization (P_r) and coercive field (E_c) are plotted in Fig. 4(b). Obviously, with increasing x value, these parameters increase slowly, reach the maximum near $x = 0.05$ with the largest P_{\max} , P_r , and E_c of 14.3 $\mu\text{C}/\text{cm}^2$, 7.3 $\mu\text{C}/\text{cm}^2$, and 16.3 kV/cm, respectively, and then, decreases sharply to 12.4 $\mu\text{C}/\text{cm}^2$, 0.9 $\mu\text{C}/\text{cm}^2$, and 3.3 kV/cm for the P_{\max} , P_r , and E_c , respectively, of the composition with $x = 0.065$.

The introduction of BF not only suppresses the tetragonal phase and enhances the pseudocubic phase, which is detrimental for ferroelectric property but also leads to significantly increased grain size, which is positive for ferroelectric property because of small grain size meaning large amount of grain boundary, and grain boundary will lead to polarization discontinuity between grains and hence decreased polarization.²⁴ The above two competing effects should be responsible for the observed composition-dependent ferroelectric property: when $x \leq 0.05$, the positive effect dominates, whereas when $x > 0.05$, the detrimental effect tends to be dominative.

The room temperature bipolar S - E curves of all compositions are shown in Fig. 5. With the applied field of 80 kV/cm, all ceramics have butterfly-shaped S - E curves, indicating the ferroelectric nature. With increasing x from 0 to 0.05, the butterfly shape become obvious, reaching the best shape

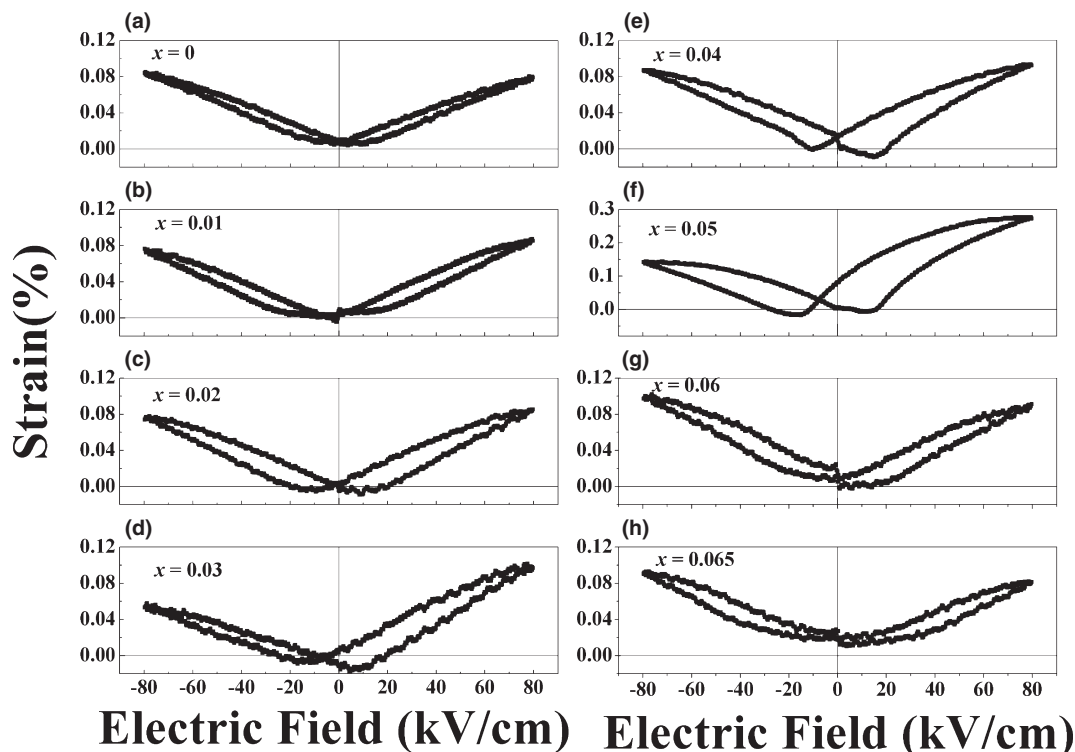


Fig. 5. Bipolar S - E curves of the $(1-x)\text{BCT}-x\text{BF}$ ($x = 0-0.065$) ceramics.

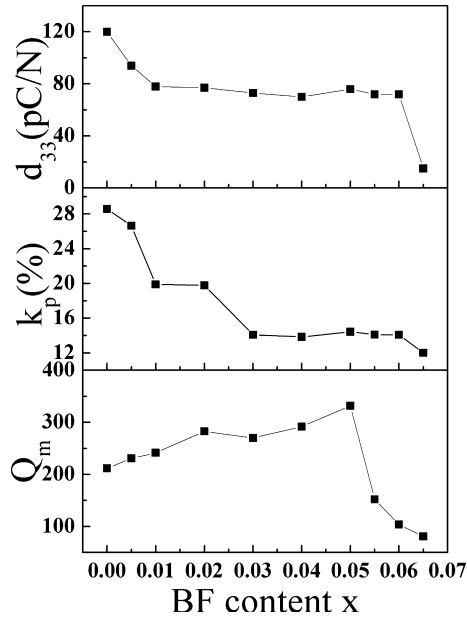


Fig. 6. d_{33} , k_p , and Q_m Values of the $(1-x)\text{BCT}-x\text{BF}$ ceramics as a function of BF content.

with largest strain value, and with further increasing x , the butterfly shape tends to diminish and the strain decreases. It should be noted that the composition dependence of $S-E$ curves is consistent with that of $P-E$ loops.

Figure 6 shows the room temperature piezoelectric coefficient (d_{33}), planar mode electromechanical coupling coefficient (k_p), and mechanical quality factor (Q_m) of BCT-BF ceramics as a function of BF content. It can be observed that d_{33} and k_p decreased simultaneously with increasing BF content, which may be attributed to the phase transition from tetragonal to pseudocubic symmetry and the ferroelectric-paraelectric phase transition temperature is decreased to near room temperature with increasing x , Q_m reached the maximum of 331.84 in the composition with $x = 0.05$, then decreased sharply with increasing x , which should be attributed to the composition dependence ferroelectrics, as indicated by that of $P-E$ and $S-E$.

IV. Conclusions

Lead-free piezoelectric ceramics $(1-x)\text{Ba}_{0.70}\text{Ca}_{0.30}\text{TiO}_3-x\text{BiFeO}_3$ have been prepared and the effects of BF content on the microstructure and electrical properties of BCT ceramics have been investigated. It is found that the composition with $x = 0-0.06$ has coexisted tetragonal and orthorhombic phases whereas that with $x = 0.065$ has coexisted pseudocubic and orthorhombic phases. With increasing x , the grain size of tetragonal phases becomes larger, and the ferroelectric-paraelectric phase transition temperature decreases monotonically from 128°C to 50°C, accompanied by slightly enhanced ferroelectric relaxor behavior, which can be attributed to the disruption of long-range dipolar interaction due to substitution of A-site Bi^{3+} and B-site Fe^{3+} . The composition-dependent ferroelectric and piezoelectric parameters are discussed based on the structures. These results may be helpful for

understanding and stimulating further work on electric properties of BaTiO_3 -related lead-free materials.

Acknowledgments

This work was supported by the National Nature Science Foundation of China (10704021, 51102062, and 11174127), the Key Scientific and Technological Project of Harbin (grant no. 2009AA3BS131).

References

- B. Jaffe, W. R. Cook, and H. Jaffe, *Piezoelectric Ceramics*. Academic Press, London, 1971.
- W. F. Liu and X. B. Ren, "Large Piezoelectric Effect in Pb-Free Ceramics," *Phys. Rev. Lett.*, **103** [25] 257602-4 (2009).
- W. Li, Z. J. Xu, R. Q. Chu, P. Fu, and G. Z. Zang, "Large Piezoelectric Coefficient in $(\text{Ba}_{1-x}\text{Ca}_x)(\text{Ti}_{0.96}\text{Sn}_{0.04})\text{O}_3$ Lead-Free Ceramics," *J. Am. Ceram. Soc.*, **94** [12] 4131-3 (2011).
- W. Li, Z. J. Xu, R. Q. Chu, P. Fu, and G. Z. Zang, "Piezoelectric and Dielectric Properties of $(\text{Ba}_{1-x}\text{Ca}_x)(\text{Ti}_{0.95}\text{Zr}_{0.05})\text{O}_3$ Lead-Free Ceramics," *J. Am. Ceram. Soc.*, **93** [10] 2942-4 (2010).
- X. S. Wang, H. Yamada, K. Nishikubo, and C. N. Xu, "Electrostrictive Properties of Pr-Doped BaTiO_3 - CaTiO_3 Ceramics," *Jpn. J. Appl. Phys.*, **45**, 813-6 (2006).
- X. S. Wang, C. N. Xu, H. Yamada, K. Nishikubo, and X. G. Zheng, "Electro-Mechano-Optical Conversions in Pr^{3+} Doped BaTiO_3 - CaTiO_3 Ceramics," *Adv. Mater.*, **17** [10] 1254-8 (2005).
- S. N. Yun and X. L. Wang, "Dielectric Properties of Bismuth Doped $\text{Ba}_{1-x}\text{Ca}_x\text{TiO}_3$ Ceramics," *Mater. Lett.*, **60**, 2211-3 (2006).
- X. S. Wang, H. Yamada, and C. N. Xu, "Large Electrostriction near the Solubility Limit in BaTiO_3 - CaTiO_3 Ceramics," *Appl. Phys. Lett.*, **86**, 022905, 3pp (2005).
- M. R. Panigrahi and S. Panigrahi, "Structural Analysis of 100% Relative Intense Peak of $\text{Ba}_{1-x}\text{Ca}_x\text{TiO}_3$ Ceramics by X-ray powder Diffraction Method," *Physica B*, **405**, 1787-91 (2010).
- S. Jayanthi and T. R. N. Kuttly, "Extended Phase Homogeneity and Electrical Properties of Barium Calcium Titanate Prepared by the Wet Chemical Methods," *Mater. Sci. Eng. B*, **110**, 202-12 (2004).
- X. R. Cheng and M. R. Shen, "Enhanced Spontaneous Polarization in Sr and Ca Co-Doped BaTiO_3 Ceramics," *Solid State Commun.*, **141** [11] 587-90 (2007).
- D. S. Kang, M. S. Han, S. G. Lee, and S. H. Song, "Dielectric and Pyroelectric Properties of Barium Strontium Calcium Titanate Ceramics," *J. Eur. Ceram. Soc.*, **23** [3] 515-8 (2003).
- N. Yasuda, H. Ohwa, and S. Asano, "Dielectric Properties and Phase Transitions of $\text{Ba}(\text{Ti}_{1-x}\text{Sn}_x)\text{O}_3$ Solid Solution," *Jpn. J. Appl. Phys.*, **35**, 5099-103 (1996).
- A. Chen, J. Zhi, and Y. Zhi, "Ferroelectric Relaxor $\text{Ba}(\text{Ti,Ce})\text{O}_3$," *J. Phys. Condens. Matter*, **14**, 8901-12 (2002).
- X. G. Tang, K. H. Chew, and H. L. W. Chan, "Diffuse Phase Transition and Dielectric Tunability of $\text{Ba}(\text{Zr}_{1-x}\text{Ti}_x)\text{O}_3$ Relaxor Ferroelectric Ceramics," *Acta Mater.*, **52** [17] 5177-83 (2004).
- T. Mitsui and W. B. Westphal, "Dielectric and X-Ray Studies of $\text{Ca}_{1-x}\text{Ba}_x\text{TiO}_3$ and $\text{Ca}_{1-x}\text{Sr}_x\text{TiO}_3$," *Phys. Rev.*, **124** [5] 1354-9 (1961).
- H. X. Fu and R. E. Cohen, "Polarization Rotation Mechanism for Ultrahigh Electromechanical Response in Single-Crystal Piezoelectrics," *Nature (London)*, **403**, 281-3 (2000).
- G. Catalan and J. F. Scott, "Physics and Applications of Bismuth Ferrite," *Adv. Mater.*, **21** [24] 2463-85 (2009).
- J. G. Wu and J. Wang, "BiFeO₃ Thin films of (111)-Orientation Deposited on SrRuO_3 Buffered Pt/TiO₂/SiO₂/Si(100) Substrates," *Acta Mater.*, **58**, 1688-97 (2010).
- J. G. Wu, W. J. Wu, and D. Q. Xiao, "(Ba, Ca)(Ti, Zr)O₃ Lead-Free Piezoelectric Ceramics," *Curr. Appl. Phys.*, **12**, 534-8 (2012).
- A. Ullah, C. W. Ahn, A. Hussain, S. Y. Lee, and I. W. Kim, "Phase Transition, Electrical Properties, and Temperature-Intensive Large Strain in BiAlO₃-Modified Bi_{0.5}(Na_{0.75}K_{0.25})_{0.5}TiO₃ Lead-Free Piezoelectric Ceramics," *J. Am. Ceram. Soc.*, **94** [11] 3915-21 (2011).
- S. Mahajan, O. P. Thakur, D. K. Bhattacharya, and K. Sreenivas, "Ferroelectric Relaxor Behaviour and Impedance Spectroscopy of Bi₂O₃-Doped Barium Zirconium Titanate Ceramics," *J. Phys. D Appl. Phys.*, **42**, 065413, 10pp (2009).
- T. Maiti, R. Guo, and A. S. Bhalla, "The Evolution of Relaxor Behavior in Ti⁴⁺ Doped BaZrO_3 Ceramics," *J. Appl. Phys.*, **100**, 114109, 6pp (2006).
- P. A. Jha and A. K. Jha, "Influence of Processing Conditions on the Grain Growth and Electrical Properties of Barium Zirconate Titanate Ferroelectric Ceramics," *J. Alloy. Compd.*, **513**, 580-5 (2012). □